mathematics

MDPI

Article

Input Estimation for Repetitive-Motion Plants via ILC Subject to Quantization Errors and Packet Dropouts

Haixu Niu [1], Zhichao Ding [2] and Lixun Huang [3,*]

[1] College of Physical Education, Henan University of Technology, Zhengzhou 450000, China; niuhaixu@haut.edu.cn
[2] School of Computer Science and Artificial Intelligence, Zhengzhou University of Light Industry, Zhengzhou 450000, China; dzc_zzuli@163.com
[3] School of Electronics and Information, Zhengzhou University of Light Industry, Zhengzhou 450000, China
* Correspondence: shuhlx@zzuli.edu.cn

Abstract

Quantization errors and packet dropouts in noisy communication channels degrade the convergence performance of repetitive-motion plants under iterative learning control (ILC). Different from existing works focusing on the redesign of ILC schemes, this paper regards the ILC-generated input as the iteration-domain state of the learning process, and proposes an estimation approach to reconstruct the actual input. Provided that the basic ILC scheme achieves convergence under ideal communication conditions free of quantization and packet dropouts, the proposed estimator mitigates the plant-side input deviation via input reconstruction in the presence of such disturbances in input–output channels. Simulation results illustrate the potential of the reconstructed input to improve the tracking performance of the controlled plant under such channel disturbances.

Keywords: input estimation; repetitive-motion plant; iterative learning control; quantization error; packet dropout

MSC: 93B47; 93E11

1. Introduction

1.1. Motivation

With the development of information and communication technologies, the concept of networked control systems has emerged. These are spatially distributed systems in which communication between sensors, actuators, and controllers is facilitated by a shared network [1]. Therefore, networked control systems offer advantages such as easy installation, low maintenance costs, and widespread applicability. These merits have led to their use in areas including robot-assisted telerehabilitation for sports-related and other injuries [2], control collaboration [3], and microseismic event detection [4]. In particular, for upper-limb rehabilitation plants and other similar systems operating repeatedly within a network, the iterative learning control (ILC) strategy serves as a promising approach, as it only requires limited prior knowledge of the controlled plants to achieve precise tracking of desired trajectories [5].

It is evident that unreliable wired or wireless networks pose new challenges in ensuring the convergence of plants controlled by ILC controllers through networks. Specifically, because the bandwidth of wireless channels is limited, input and output data often need to be quantized before transmission to reduce the transmission volume [6–10]. As a result,

Check for updates

Received: 17 September 2026
Revised: 27 October 2026
Accepted: 28 October 2026
Published: 1 November 2026

Copyright: © 2026 by the authors. Licensee MDPI, Basel, Switzerland. This article is an open access article distributed under the terms and conditions of the Creative Commons Attribution (CC BY) license.

quantization errors occur at the transmitters. Furthermore, due to the time-varying nature of wireless noisy channels, the channel gain undergoes random fading, which causes packet dropouts when the gain fades too much.

To overcome the challenge posed by communication constraints, common methods involve designing new ILC controllers [11–15]. Two drawbacks can be identified. Firstly, the designed controller can only be used for specific plants. Secondly, the converged input may be disturbed again during transmission from controllers to plants [16,17]. Meanwhile, considerable attention has been devoted to research on state estimation for networked linear repetitive processes. Related works provide new insights: assuming the ILC controller is well-designed to guarantee system convergence under ideal communication conditions, we can regard the input produced by ILC controllers as the process state to be estimated, adopt an estimation method to reconstruct this input, and then use the estimated input to actuate the controlled plant. In this way, not only can the universality of the control scheme be enhanced, but also the convergence of the input applied to the plant side can be guaranteed.

However, the existing state estimation methods for networked linear repetitive processes cannot be directly applied to estimate the input produced by ILC controllers. The gap causing this issue lies in the fact that the linear repetitive processes considered in existing works are recursive in the time domain. Although the input generating process of the ILC controller may be linear, it is recursive in the iteration domain. A few studies have investigated state estimation for iteration-domain repetitive processes, e.g., ref. [17], yet their channel models only consider disturbances occurring inside communication channels and ignore pre-transmission quantization distortion at transmitters. Furthermore, although the multiplicative quantization noise and Bernoulli packet dropout are statistically independent random variables, their combined multiplicative effect introduces coupled perturbation terms within the state dynamics, which is not considered in ref. [17]. To address such a gap, this paper focuses on developing estimation methods tailored for the iterative repetitive process (IRP) of ILC controllers. These methods aim to provide accurate inputs to the plant, thereby mitigating the adverse effects of quantization errors and packet dropouts in noisy channels.

1.2. Related Works

Quantization methods employed to address bandwidth limitations typically include uniform quantization [18–20] and logarithmic quantization [21–23], the main distinction between them lies in the setting of quantization intervals. As to the former, the quantization region is divided into equally spaced intervals, each corresponding to a constant discrete value. In contrast, the quantization intervals in logarithmic quantization vary with the change of signal samples, offering this method a broader range of applications. Additionally, these two quantization methods affect transmitted data differently [24]. To be specific, the uniform quantization error was also modeled as additive white noise. For example, in [25], the authors investigated the design of a network recursive filter with uniform quantization and noted that the quantization error can be modeled as additive noise with a constant step size. In ref. [18], the authors modeled the quantization errors in resilient filtering for repetitive processes as additive noise and ensured that the variance of filtering errors remained below a certain upper bound. In contrast to the additive noise model for uniform quantization errors, logarithmic quantization errors are typically modeled as multiplicative noise using the sector-bound method [26]. This modeling method can also be found in ref. [23], where the authors addressed the H_∞ filtering problem for discrete-time periodic Markov jump systems with quantized measurements and packet dropout compensation. A static logarithmic quantizer with mode-dependent characteristics is used to quantize the measurement outputs, and the quantization error is modeled as multiplicative noise.

In addition to quantization errors at transmitters, data may also experience random dropouts during wireless transmission due to channel gain fading. Methods to model packet dropouts primarily include the Bernoulli model, random sequence model, and Markov chain model. Among these, the Bernoulli model represents packet dropouts as a binary random variable with a clear probabilistic distribution, assuming that packet dropout events are independent of one another [27–30]. In contrast to the Bernoulli model, which relies on the probability distribution of random variables, the random sequence model defines a sequence of bounded length to simulate the positions of packet dropouts. This method is suitable for describing the continuity of packet dropouts but requires the number of consecutive data dropouts to be finite [31]. Additionally, the Markov chain model treats packet dropouts as a Markov process [32,33], enabling a rigorous convergence analysis in the mean square sense. For example, in [32], to address the convergence of linear stochastic systems with general packet dropouts, the authors used the Markov model to describe the update process of both computed and real inputs as a Markov chain. In the sliding mode control problem of a Markov jump repeated system with packet dropouts in [33], the authors modeled packet dropouts using a random variable following a Markov process and ensured the robust asymptotic mean square stability of the system. The three models mentioned above typically handle the effects of packet dropouts in either the iteration or the time domain. Iterative domain compensation uses data from the previous iteration. For instance, in [34], for the problem of a nonlinear discrete-time switching system with random packet dropouts, the authors used data from the previous iteration as a substitute for the lost data, ensuring the stability of the system output. In contrast to iterative domain compensation, time domain compensation uses data from the previous time step within the same iteration. In [35], for the problem of convergence in an ILC system affected by packet dropouts and noise, the authors used time domain compensation to mitigate the effects of packet dropouts on the system.

Data transmitted over wireless channels not only experiences random packet dropouts but also suffers from noise interference [36]. Specifically, during iterative processes, the impact of channel noise can accumulate over time as the system repeats its operations. For example, in [37], the authors pointed out that as the number of iterations tends to infinity, the effects of noise are continuously amplified. Furthermore, the impact of input channel noise on system convergence is significantly greater than that of output channel noise. To mitigate the effects of channel noise, filtering techniques have been widely studied as an effective countermeasure. For example, in [38], the authors designed a filter for networked ILC systems to recover the true input sent by controllers through noisy channels. In [39], the authors proposed an adaptive periodic disturbance observer to suppress the effects of both fundamental and harmonic components, as well as handle disturbances with frequency variations. In [40], the authors present a collaborative design method for decentralized filtering of interconnected systems based on a T-S fuzzy model, aimed at optimizing network resource usage while maintaining the desired H_∞ filtering performance.

1.3. Core Contributions

The shortcomings of the above research can be summarized as follows. First, relatively few existing studies simultaneously consider the quantization error before signal transmission and packet dropout during signal transmission [15,23,29,30]. Second, for closed-loop networked ILC systems, communication constraints represented by packet dropout may exist not only in the output channel but also in the input channel [11,13,15,34]. Third, many previous studies concentrate on designing learning strategies that cannot guarantee the convergence performance of the inputs received by the plant [11–15,32,34]. Finally, state estimation research subject to communication constraints mainly focuses on conventional

non-repetitive processes [19,21,22,24,25]. Even for repetitive process-based results, most existing methods only address time-domain state recursion [18,23,29,30], whereas estimation for the IRP is rarely investigated [16,17,38]. Nevertheless, it should be noted that the proposed method also cannot provide theoretical guarantees for end-to-end tracking performance under network impairments. Table 1 provides a qualitative comparison of representative existing literature with respect to the communication constraints considered.

Table 1. Summary of representative related works.

Research Type	Refs.	PD_{in}	PD_{out}	QE	MN	AN
Non-repetitive process state estimation	[19]			✓		
	[21]			✓		
	[22]			✓		
	[24]			✓		
	[25]			✓		
Repetitive process state estimation (Time-domain)	[18]			✓		
	[23]		✓	✓		
	[29]		✓	✓		
	[30]		✓	✓		
Repetitive process state estimation (Iteration-domain)	[16]	✓	✓			✓
	[17]				✓	✓
	[38]	✓	✓			✓
ILC controller design	[11]	✓	✓			
	[12]		✓			
	[13]	✓	✓			
	[14]		✓			
	[15]	✓	✓	✓		
	[32]		✓			
	[34]	✓	✓			

✓: the impairment is considered; blank cell means the impairment is not addressed; PD_{in}: input-channel packet dropout; PD_{out}: output-channel packet dropout; QE: Quantization error; MN: Multiplicative noise; AN: Additive noise.

To enhance the convergence of ILC systems subject to quantization errors and packet dropouts in noisy input and output channels, this paper approaches the problem from the perspective of input estimation rather than controller design. The main merit of this input-estimation scheme lies in two facts: first, it only requires knowledge of the ILC learning strategy and channel statistics; second, it avoids redesigning the ILC updating law for network imperfections. In short, the core contributions of this paper are as follows:

1. A unified modeling framework is constructed for the networked ILC systems subject to quantization and packet dropouts, where the ILC-produced input is defined as the IRP state to be estimated.
2. An estimator based on innovation analysis is designed to reconstruct the control input at the plant side and mitigate the adverse effects induced by network constraints.

The structure of the remainder of the paper is as follows: Section 2 formulates the initial problem, Section 3 presents the estimator design and its corresponding formula derivation, Section 4 provides simulation verification of the designed estimator, and Section 5 concludes the paper.

Notations: The hat symbol $\hat{\cdot}$ over a variable denotes its estimated value; the tilde symbol $\tilde{\cdot}$ over a variable represents its estimation error; the overline $\bar{\cdot}$ on a variable indicates its statistical expectation. The superscripts -1 and T denote matrix inverse and matrix transpose, respectively. $\mathbb{E}\{\cdot\}$ stands for the mathematical expectation operator for random variables.

The operator $\Delta\{\cdot\}$ represents zero-mean stochastic deviation, defined as $\Delta\mathbf{A} = \mathbf{A} - \overline{\mathbf{A}}$, where $\overline{\mathbf{A}} = \mathbb{E}\{\mathbf{A}\}$. Matrices I and 0 represent the identity matrix and zero matrix with appropriate dimensions.

2. Problem Formulation

Since the input estimation only requires prior knowledge of the controller and communication channel, rather than knowledge of the controlled plant, the IRP of the proportional ILC scheme is described by the following iteration update rule:

$$u_{k+1}(t) = u_k(t) + \Gamma e_k^r(t+1) \tag{1}$$

where $u_{k+1}(t)$ is the input generated by the controller and regarded as the process state of the IRP; $e_k^r(t+1)$ denotes the output error data received by the controller and treated as the process input of the IRP; Γ is the learning gain; k represents the iteration index; t denotes the discrete time instant within each iteration, with $t \in [0, T]$; and T is the time length of one iteration period.

To control plants through communication channels, the produced input data $u_{k+1}(t)$ needs to be sent to the remote estimator. To data transmission, the limitation of bandwidth should be considered. A common method is to quantify the data before transmission to reduce the data volume. Moreover, due to the levels vary in logarithmic quantizers, the performance of which is usually superior to that of uniform quantizers. Therefore, this paper uses the logarithmic quantizer defined as:

$$Q(f(t)) = \begin{cases} l^j, & \text{if} \frac{l^j}{1+\psi} < f(t) < \frac{l^j}{1-\psi} \\ 0, & \text{if} f(t) = 0 \\ -Q(-f(t)), & \text{if} f(t) < 0 \end{cases} \tag{2}$$

where $f(t)$ is the input for quantizers, $Q(f(t))$ is the output, ρ represents the quantization density and satisfies $0 < \rho < 1$, $\psi = \frac{1-\rho}{1+\rho}$, $l^j = \rho^j l^0$ is the quantization level, and the initial state of quantizers satisfies $l^0 > 0$.

The relationship between the input and output of quantizers can be described as:

$$Q(f(t)) = f(t) + Q_e(t) \tag{3}$$

where $Q_e(t)$ represents the quantization error. According to the sector interval boundary method given in [26], any quantization function $Q(f(t))$ can be expressed as:

$$Q(f(t)) = (1 + \xi(t))f(t) \tag{4}$$

where $|\xi(t)| \leq \psi$. Therefore, the quantization error can be expressed as:

$$Q_e(t) = \xi(t)f(t) \tag{5}$$

Note that the sector-bound property $|\xi(t)| \leq \psi$ in (4) is a deterministic conclusion derived in [26], which only provides the upper bound for the relative quantization error without any statistical characterization. To facilitate stochastic performance analysis, an additional statistical assumption is adopted: when the input signal $f(t)$ is sufficiently rich and traverses multiple quantization intervals, the relative multiplicative noise $\xi(t)$ is assumed to be zero-mean and uniformly distributed over $[-\psi, \psi]$. For such a zero-mean uniform random variable, its variance is given by

$$\mathrm{Var}(\xi(t)) = \frac{\psi^2}{3} \tag{6}$$

It should be noted that $Q_e(t) = \xi(t)f(t)$ is signal-dependent, whose statistical property is coupled with the input signal $f(t)$. This assumption serves as a feasible engineering approximation under the condition that the amplitude of $f(t)$ is much larger than the quantization step and different quantization cells are sufficiently excited. It is worth highlighting that the uniform-distribution assumption is only utilized to compute the first- and second-order moments of the relative multiplicative quantization noise. The subsequent derivation of the proposed estimator follows the linear minimum-mean-square estimation framework, which only requires these moments and does not rely on the exact probability distribution of multiplicative noise.

In addition to the quantization errors that occur before transmission, quantized data would be lost randomly in noisy channels varying in time. Taking these uncertainties into account comprehensively, the data transmission can be described as:

$$e_k^r(t) = a_k(t)[1 + \omega_k(t)]e_k(t) + (1 - a_k(t))e_{k-1}^r(t) + m_k(t) \tag{7}$$

$$u_k^r(t) = b_k(t)[1 + \sigma_k(t)]u_k(t) + (1 - b_k(t))u_{k-1}^r(t) + n_k(t) \tag{8}$$

where $e_k(t)$ is the output error data of controlled plants, $u_k^r(t)$ is the input received by plants. $\omega_k(t)$ and $\sigma_k(t)$ are multiplicative coefficients induced by quantization errors, $n_k(t)$ and $m_k(t)$ are additive noises in wireless channels. $a_k(t)$ and $b_k(t)$ follow Bernoulli distributions to describe packet dropouts. For convenience in discussion, the following assumptions are considered.

Assumption 1. *The means of $a_k(t)$ and $b_k(t)$ satisfy $\mathbb{P}\{a_k(t) = 1\} = \bar{a}$, $0 < \bar{a} \leq 1$ and $\mathbb{P}\{b_k(t) = 1\} = \bar{b}$, $0 < \bar{b} \leq 1$.*

Assumption 2. *$\omega_k(t)$, $\sigma_k(t)$, $m_k(t)$ and $n_k(t)$ are mutually independent zero-mean random variables. The multiplicative quantization-related noises $\omega_k(t)$ and $\sigma_k(t)$ have variances $Q_\omega = Q_\sigma = \psi^2/3$; $m_k(t)$ and $n_k(t)$ follow Gaussian distributions with variances Q_m and Q_n, respectively.*

It should be noted that the above Bernoulli packet-dropout assumption supposes independent dropout events across different time instants. Practical wireless communication channels may produce correlated burst dropouts, time delays and out-of-order packets, which are not characterized within the present theoretical framework. Additionally, the multiplicative noise description for logarithmic quantization is a stochastic equivalent assumption for theoretical analysis. Real quantization error is deterministic and signal-dependent. This approximation is effective when the signal amplitude is away from the quantizer dead zone, and its conservativeness will increase when signals are close to zero. Furthermore, channel noises are supposed to be statistically independent across iterations in our analysis; iteration-invariant or iteration-correlated disturbances encountered in practical repetitive systems are not covered by the present theoretical framework.

Our motivation for introducing the input estimator to improve the ILC performance of repetitive processes under quantization and packet-dropout constraints is as follows. If the adopted ILC law can guarantee output convergence under ideal communication, accurate reconstruction of the control signal sent by the ILC controller can compensate input-channel disturbances, so that satisfactory output convergence can still be achieved even when both input and output channels suffer from various interferences. To this end, an input estimator is deployed at the plant side to precisely reconstruct the control input transmitted from the ILC controller. The block diagram of the whole system is shown in Figure 1. This estimator receives the disturbed control signal transmitted over the input channel and reconstructs the estimated input $\hat{\boldsymbol{u}}_{k|k}(t)$ for the plant actuator. Notably, the ILC update law remains

unchanged; the controller still uses the corrupted tracking error fed back from the output channel for iterative updates.

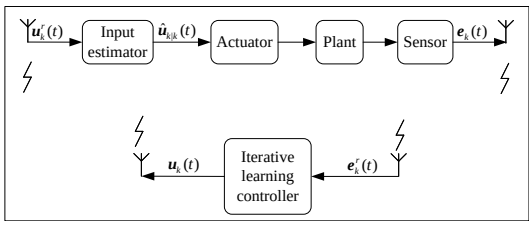


Figure 1. Block diagram of the networked ILC system with the proposed input estimator.

3. Proposed Estimation Method

3.1. Estimation Model Construction

By organizing the produced input of IRPs and the received input data and output error data into a vector, a model would be constructed as follows:

$$\underline{x}_{k+1}(t) = \underline{\gamma}_k \underline{x}_k(t) + \underline{\eta}_{1,k} \underline{u}_k(t) + \underline{\eta}_{2,k} \underline{w}_k(t) \tag{9}$$

$$\underline{y}_k(t) = \underline{\delta}_k \underline{x}_k(t) + \underline{v}_k(t) \tag{10}$$

where

$$\underline{x}_{k+1}(t) = col\{u_{k+1}(t), u_k^r(t), e_k^r(t)\},$$
$$\underline{u}_k(t) = e_k(t+1),$$
$$\underline{y}_k(t) = u_k^r(t),$$
$$\underline{w}_k(t) = col\{m_k(t), n_k(t)\},$$
$$\underline{v}_k(t) = n_k(t),$$
$$\underline{\gamma}_k = \begin{bmatrix} I & 0 & (1-a_k(t))\Gamma \\ b_k(t)(1+\sigma_k(t))I & (1-b_k(t))I & 0 \\ 0 & 0 & (1-a_k(t))I \end{bmatrix},$$
$$\underline{\eta}_{1,k} = \begin{bmatrix} a_k(t)(1+\omega_k(t))\Gamma \\ 0 \\ a_k(t)(1+\omega_k(t))I \end{bmatrix}, \underline{\eta}_{2,k} = \begin{bmatrix} \Gamma & 0 \\ 0 & I \\ I & 0 \end{bmatrix},$$
$$\underline{\delta}_k = \begin{bmatrix} b_k(t)(1+\sigma_k(t))I & (1-b_k(t))I & 0 \end{bmatrix}.$$

According to Assumptions, we can get $E\{a_k(t)^2\} = \bar{a}$, $E\{b_k(t)^2\} = \bar{b}$, $Q_{\underline{w}} = \begin{bmatrix} Q_m & 0 \\ 0 & Q_n \end{bmatrix}$, $Q_{\underline{v}} = Q_n$, and $Q_s = E\{\underline{w}_k(t)\underline{v}_k(t)^T\} = \begin{bmatrix} 0 \\ Q_n \end{bmatrix}$.

Remark 1. *Packet dropouts, quantization-induced multiplicative noises and channel additive noises are all embedded into the augmented iteration-domain state-space model constructed in Equations (9) and (10). Packet dropouts are characterized by Bernoulli-type binary random variables $a_k(t)$ and $b_k(t)$ with given successful-transmission probabilities. For multiplicative quantization noise, the uniform-distribution assumption is an engineering approximation under sufficiently rich input excitation and is only adopted to compute its statistical moments. The additive channel noises are modeled as zero-mean Gaussian variables. All above random terms are assumed mutually uncorrelated. The proposed linear minimum mean square error (LMMSE) estimator jointly handles these three types of network impairments by exploiting their statistical first- and second-order moments.*

3.2. Estimator Design

Before designing the estimator, we first define the mean and deviation values of the filtering model parameters. Specifically, the overline represents the expectation of a random variable, and $\Delta(\cdot)$ denotes the corresponding deviation from its expectation. The notations are defined as: $\overline{\underline{\gamma}}_k = \mathbb{E}\{\underline{\gamma}_k\}$, $\overline{\underline{\eta}}_{1,k} = \mathbb{E}\{\underline{\eta}_{1,k}\}$, $\overline{\underline{\eta}}_{2,k} = \mathbb{E}\{\underline{\eta}_{2,k}\}$, $\overline{\underline{\delta}}_k = \mathbb{E}\{\underline{\delta}_k\}$, $\Delta\underline{\gamma}_k = \underline{\gamma}_k - \overline{\underline{\gamma}}_k$, $\Delta\underline{\eta}_{1,k} = \underline{\eta}_{1,k} - \overline{\underline{\eta}}_{1,k}$, $\Delta\underline{\eta}_{2,k} = \underline{\eta}_{2,k} - \overline{\underline{\eta}}_{2,k}$, $\Delta\underline{\delta}_k = \underline{\delta}_k - \overline{\underline{\delta}}_k$. Two lemmas are provided as follows.

Lemma 1. *The following results can be derived for the estimation model*

$$\begin{aligned}
\overline{\underline{\gamma}}_k &= \begin{bmatrix} I & 0 & (1-\overline{a})\Gamma \\ \overline{b}I & (1-\overline{b})I & 0 \\ 0 & 0 & (1-\overline{a})I \end{bmatrix}, \ \overline{\underline{\eta}}_{1,k} = \begin{bmatrix} \overline{a}\Gamma \\ 0 \\ \overline{a}I \end{bmatrix}, \\
\overline{\underline{\eta}}_{2,k} &= \begin{bmatrix} \Gamma & 0 \\ 0 & I \\ I & 0 \end{bmatrix}, \ \overline{\underline{\delta}}_k = \begin{bmatrix} \overline{b}I & 0 & 0 \end{bmatrix}.
\end{aligned} \tag{11}$$

$$\begin{aligned}
\Delta\underline{\gamma}_k &= \left(b_k(t) - \overline{b}\right)\Xi_1 + b_k(t)\sigma_k(t)\Xi_2 + (a_k(t) - \overline{a})\Xi_3, \\
\Delta\underline{\eta}_{1,k} &= (a_k(t) + a_k(t)\omega_k(t) - \overline{a})\Xi_4, \\
\Delta\underline{\eta}_{2,k} &= 0, \\
\Delta\underline{\delta}_k &= \left(b_k(t) - \overline{b}\right)\Xi_5 + b_k(t)\sigma_k(t)\Xi_6.
\end{aligned} \tag{12}$$

where $\Xi_1 = \begin{bmatrix} 0 & 0 & 0 \\ I & -I & 0 \\ 0 & 0 & 0 \end{bmatrix}$, $\Xi_2 = \begin{bmatrix} 0 & 0 & 0 \\ I & 0 & 0 \\ 0 & 0 & 0 \end{bmatrix}$, $\Xi_3 = \begin{bmatrix} 0 & 0 & -\Gamma \\ 0 & 0 & 0 \\ 0 & 0 & -I \end{bmatrix}$, $\Xi_4 = \begin{bmatrix} \Gamma \\ 0 \\ I \end{bmatrix}$, $\Xi_5 = \begin{bmatrix} I & -I & 0 \end{bmatrix}$, *and* $\Xi_6 = \begin{bmatrix} I & 0 & 0 \end{bmatrix}$.

Proof. Equation (11) follows directly from taking expectation on defined stochastic parameters, and Equation (12) follows directly from (11). □

Lemma 2. *Defining* $\overline{\underline{u}}_k = E\{\underline{u}_k\}$, $\overline{\underline{x}}_k = E\{\underline{x}_k\}$, *for the model described in* (9) *and* (10), *the second-order origin moment* $q_k = E\{\underline{x}_k\underline{x}_k^T\}$ *satisfies the recursion as:*

$$\begin{aligned}
q_{k+1} &= E\{\underline{x}_{k+1}\underline{x}_{k+1}^T\} \\
&= \overline{\underline{\gamma}}_k q_k \overline{\underline{\gamma}}_k^T + \overline{\underline{\gamma}}_k E\{\underline{x}_k\underline{u}_k^T\}\overline{\underline{\eta}}_{1,k}^T + \overline{\underline{\eta}}_{1,k} E\{\underline{u}_k\underline{x}_k^T\}\overline{\underline{\gamma}}_k^T + \overline{\underline{\eta}}_{1,k}\overline{\underline{u}}_k\overline{\underline{u}}_k^T\overline{\underline{\eta}}_{1,k}^T \\
&+ \left(\overline{b} - \overline{b}^2\right)\Xi_1 q_k \Xi_1^T + \overline{b}Q_\sigma\Xi_2 q_k \Xi_2^T + \left(\overline{a} - \overline{a}^2\right)\Xi_3 q_k \Xi_3^T \\
&+ \left(\overline{a} - \overline{a}^2 + \overline{a}Q_\omega\right)\Xi_4\overline{\underline{u}}_k\overline{\underline{u}}_k^T\Xi_4^T + \overline{\underline{\eta}}_{2,k}Q_{\underline{w}}\overline{\underline{\eta}}_{2,k}^T
\end{aligned} \tag{13}$$

Proof. Equation (9) can be rewritten as:

$$\underline{x}_{k+1}(t) = \left(\overline{\underline{\gamma}}_k + \Delta\underline{\gamma}_k\right)\underline{x}_k(t) + \left(\overline{\underline{\eta}}_{1,k} + \Delta\underline{\eta}_{1,k}\right)\underline{u}_k(t) + \left(\overline{\underline{\eta}}_{2,k} + \Delta\underline{\eta}_{2,k}\right)\underline{w}_k(t)$$

Accordingly, the second geometric moment of state could be expressed as

$$\begin{aligned}
q_{k+1} &= \overline{\underline{\gamma}}_k q_k \overline{\underline{\gamma}}_k^T + \overline{\underline{\gamma}}_k E\{\underline{x}_k\underline{u}_k^T\}\overline{\underline{\eta}}_{1,k}^T + \overline{\underline{\eta}}_{1,k} E\{\underline{u}_k\underline{x}_k^T\}\overline{\underline{\gamma}}_k^T + \overline{\underline{\eta}}_{1,k}\overline{\underline{u}}_k\overline{\underline{u}}_k^T\overline{\underline{\eta}}_{1,k}^T \\
&+ E\left\{\Delta\underline{\gamma}_k q_k \Delta\underline{\gamma}_k^T\right\} + E\left\{\Delta\underline{\eta}_{1,k}\underline{u}_k\underline{u}_k^T\Delta\underline{\eta}_{1,k}^T\right\} + E\left\{\underline{\eta}_{2,k}\underline{w}_k\underline{w}_k^T\underline{\eta}_{2,k}^T\right\}
\end{aligned} \tag{14}$$

where

$$E\left\{\Delta\underline{\gamma}_k q_k \Delta\underline{\gamma}_k^T\right\} = \left(\bar{b} - \bar{b}^2\right)\Xi_1 q_k \Xi_1^T + \bar{b}Q_\sigma \Xi_2 q_k \Xi_2^T + \left(\bar{a} - \bar{a}^2\right)\Xi_3 q_k \Xi_3^T \tag{15}$$

$$E\left\{\Delta\underline{\eta}_{1,k}\underline{u}_k\underline{u}_k^T\Delta\underline{\eta}_{1,k}^T\right\} = \left(\bar{a} - \bar{a}^2 + \bar{a}Q_\omega\right)\Xi_4\overline{\underline{u}}_k\overline{\underline{u}}_k^T\Xi_4^T \tag{16}$$

$$E\left\{\underline{\eta}_{2,k}\underline{w}_k\underline{w}_k^T\underline{\eta}_{2,k}^T\right\} = \overline{\underline{\eta}}_{2,k}Q_{\underline{w}}\overline{\underline{\eta}}_{2,k}^T \tag{17}$$

Substituting Equations (15)–(17) into (14), we obtain (13). □

Based on the above preparation works, the state estimator can be designed according to the innovation analysis theory. We define Φ_k as the innovation sequence with covariance matrix as $\theta_k = E\{\Phi_k\Phi_k^T\}$, $K_k = E\{\underline{x}_k\Phi_k^T\}\theta_k^{-1}$ means the filter gain, $L_k = E\{\underline{x}_{k+1}\Phi_k^T\}\theta_k^{-1}$ is the prediction gain, $P_{k|k}$ and $P_{k+1|k}$ are covariance matrices of filter errors and prediction errors, $\hat{\underline{x}}_{k|k-1} = \min_{\theta_{1,k}} E\left\{\left(\theta_{1,k} - \underline{x}_k\right)(\cdot)^T\right\}$, $\hat{\underline{x}}_{k+1|k-1} = \min_{\theta_{2,k}} E\left\{\left(\theta_{2,k} - \underline{x}_k\right)(\cdot)^T\right\}$, $\hat{\underline{y}}_{k|k-1} = \min_{\theta_{3,k}} E\left\{\left(\theta_{3,k} - \underline{x}_k\right)(\cdot)^T\right\}$, where $\theta_{1,k}$, $\theta_{2,k}$, and $\theta_{3,k}$ are linear functions of $\underline{y}_1, \underline{y}_2, \ldots, \underline{y}_{k-1}$.

Theorem 1. *The estimation for the model represented in (9) and (10) can be given as*

$$\hat{\underline{x}}_{k|k} = \hat{\underline{x}}_{k|k-1} + K_k\Phi_k, \tag{18}$$

$$\hat{\underline{x}}_{k+1|k} = \hat{\underline{x}}_{k+1|k-1} + L_k\Phi_k, \tag{19}$$

$$\Phi_k = \underline{y}_k - \hat{\underline{y}}_{k|k-1}, \tag{20}$$

$$\hat{\underline{x}}_{k+1|k-1} = \overline{\underline{\gamma}}_k\hat{x}_{k|k-1} + \overline{\underline{\eta}}_{1,k}\underline{u}_k, \tag{21}$$

$$\hat{\underline{y}}_{k|k-1} = \overline{\underline{\delta}}_k\hat{\underline{x}}_{k|k-1}, \tag{22}$$

$$K_k = P_{k|k-1}\overline{\underline{\delta}}_k^T\theta_k^{-1}, \tag{23}$$

$$L_k = \left(\overline{\underline{\gamma}}_k P_{k|k-1}\overline{\underline{\delta}}_k^T + H_k\right)\theta_k^{-1}, \tag{24}$$

$$\theta_k = \overline{\underline{\delta}}_k P_{k|k-1}\overline{\underline{\delta}}_k^T + I_k, \tag{25}$$

$$\begin{aligned} P_{k+1|k} &= \left(\overline{\underline{\gamma}}_k - L_k\overline{\underline{\delta}}_k\right)P_{k|k-1}\left(\overline{\underline{\gamma}}_k - L_k\overline{\underline{\delta}}_k\right)^T \\ &+ L_kQ_mT_k^T + \Lambda_{1,k} + \Lambda_{2,k} + \Lambda_{3,k} \\ &+ \Lambda_{4,k} + \Lambda_{4,k}^T - \Lambda_{5,k} - \Lambda_{5,k}^T, \end{aligned} \tag{26}$$

$$P_{k|k} = P_{k|k-1} - K_k\theta_kK_k^T. \tag{27}$$

where

$$H_k = \left(\bar{b} - \bar{b}^2\right)\Xi_1 q_k \Xi_5^T + \bar{b}Q_\sigma \Xi_2 q_k \Xi_6^T + \overline{\underline{\eta}}_{2,k}Q_s,$$

$$I_k = \left(\bar{b} - \bar{b}^2\right)\Xi_5 q_k \Xi_5^T + \bar{b}Q_\sigma \Xi_6 q_k \Xi_6^T + Q_v,$$

$$\begin{aligned} \Lambda_{1,k} &= \left(\bar{b} - \bar{b}^2\right)(\Xi_1 - L_k\Xi_5)q_k(\Xi_1 - L_k\Xi_5)^T \\ &+ \bar{b}Q_\sigma(\Xi_2 - L_k\Xi_6)q_k(\Xi_2 - L_k\Xi_6)^T + \left(\bar{a} - \bar{a}^2\right)\Xi_3 q_k \Xi_3^T, \end{aligned}$$

$$\Lambda_{2,k} = \left(\bar{a} - \bar{a}^2 + \bar{a}Q_\omega\right)\Xi_4\overline{\underline{u}}_k\overline{\underline{u}}_k^T\Xi_4^T,$$

$$\Lambda_{3,k} = \overline{\underline{\eta}}_{2,k}Q_{\underline{w}}\overline{\underline{\eta}}_{2,k}^T,$$

$$\Lambda_{4,k} = \left(\bar{a} - \bar{a}^2\right)\Xi_3\overline{\underline{x}}_k\overline{\underline{u}}_k^T\Xi_4^T,$$

$$\Lambda_{5,k} = \overline{\underline{\eta}}_{2,k}Q_sT_k^T.$$

Proof. According to the innovation analysis theory, the estimator should satisfy Equations (18) to (20). Taking the expectation on both sides of Equations (9) and (10)

and projecting them onto the space generated by $\left(\underline{y}_1, \underline{y}_2, \ldots, \underline{y}_{k-1}\right)$, the following results can be obtained.

$$\underline{\hat{x}}_{k+1|k-1} = \overline{\gamma}_k \underline{x}_{k|k-1} + \overline{\eta}_{1,k} \underline{u}_k \tag{28}$$

$$\underline{\hat{y}}_{k|k-1} = \overline{\delta}_k \underline{\hat{x}}_{k|k-1} \tag{29}$$

Defining $\underline{\tilde{x}}_{k|k-1} = \underline{x}_k - \underline{\hat{x}}_{k-1}$ and substituting Equations (10) and (22) into (20), we obtain

$$\Phi_k = \Delta\underline{\delta}_k \underline{x}_k + \overline{\delta}_k \underline{\tilde{x}}_{k|k-1} + \underline{v}_k \tag{30}$$

It is clear that $\underline{\tilde{x}}_{k|k-1} \perp \underline{v}_k$, $\underline{x}_k \perp \underline{v}_k$, and the means of $\Delta\underline{\delta}_k$, $\underline{\tilde{x}}_{k|k-1}$, and v_k are all zero. Therefore, the innovation covariance matrix θ_k is

$$\begin{aligned} \theta_k &= E\{\Phi_k \Phi_k^T\} \\ &= \overline{\delta}_k P_{k|k-1} \overline{C}_k^T + \left(\overline{b} - \overline{b}^2\right) \Xi_5 q_k \Xi_5^T + \overline{b} Q_\sigma \Xi_6 q_k \Xi_6^T + Q_{\underline{v}} \end{aligned} \tag{31}$$

Due to $\underline{\tilde{x}}_{k|k-1} \perp \underline{\hat{x}}_{k-1}$, the filter gain K_k can be expressed as

$$K_k = E\{\underline{x}_k \Phi_k^T\} \theta_k^{-1} = P_{k|k-1} \overline{\delta}_k \theta_k^{-1}$$

Similarly, according to the definition of prediction gain, we have

$$\begin{aligned} L_k &= \mathrm{E}\{\underline{x}_{k+1} \Phi_k^T\} \theta_k^{-1} \\ &= \mathrm{E}\left\{\underline{\gamma}_k \underline{x}_k \Phi_k^T + \underline{\eta}_{1,k} \underline{u}_k \Phi_k^T + \underline{\eta}_{2,k} w_k \Phi_k^T\right\} \theta_k^{-1} \end{aligned} \tag{32}$$

Substituting Equation (30) into $E\left\{\underline{\gamma}_k \underline{x}_k \Phi_k^T\right\}$ yields

$$\begin{aligned} E\left\{\underline{\gamma}_k \underline{x}_k \Phi_k^T\right\} &= E\left\{\underline{\gamma}_k q_k \Delta\underline{\delta}_k^T\right\} + E\left\{\underline{\gamma}_k \underline{x}_k \underline{\tilde{x}}_{k|k-1}^T \underline{\delta}_k^T\right\} \\ &= \left(\overline{b} - \overline{b}^2\right) \Xi_1 q_k \Xi_5^T + \overline{b} Q_\sigma \Xi_2 q_k \Xi_6^T + \overline{\gamma}_k P_{k|k-1} \overline{\delta}_k^T \end{aligned} \tag{33}$$

Furthermore, due to $\underline{\tilde{x}}_{k|k-1} \perp \underline{\hat{x}}_{k|k-1}$, substituting Equation (30) into $\mathrm{E}\left\{\underline{\eta}_{1,k} \underline{u}_k \Phi_k^T\right\}$ and $\mathrm{E}\left\{\underline{\eta}_{2,k} \underline{w}_k \Phi_k^T\right\}$ leads to

$$\begin{aligned} \mathrm{E}\left\{\underline{\eta}_{1,k} \underline{u}_k \Phi_k^T\right\} &= \mathrm{E}\left\{\Delta\underline{\eta}_{1,k} \underline{u}_k \underline{x}_k^T \Delta\underline{\delta}_k^T\right\} \\ &= 0 \end{aligned} \tag{34}$$

$$\begin{aligned} \mathrm{E}\left\{\underline{\eta}_{2,k} \underline{w}_k \varepsilon_k^T\right\} &= \mathrm{E}\left\{\underline{\eta}_{2,k} \underline{w}_k \underline{v}_k{}^T\right\} \\ &= \overline{\eta}_{2,k} Q_s \end{aligned} \tag{35}$$

Substituting Equations (33)–(35) into (32), the prediction gain is obtained. Subtracting $\underline{\hat{x}}_{k+1|k}$ from $\underline{x}_{k+1}$, the one-step prediction error can be given as

$$\begin{aligned} \underline{\tilde{x}}_{k+1|k} &= \left(\overline{\gamma}_k - L_k \overline{\delta}_k\right) \underline{\tilde{x}}_{k|k-1} + \left(\Delta\underline{\gamma}_k - L_k \Delta\underline{\delta}_k\right) \underline{x}_k \\ &+ \Delta\underline{\eta}_{1,k} \underline{u}_k + \underline{\eta}_{2,k} \underline{w}_k - L_k \underline{v}_k \end{aligned} \tag{36}$$

As a result, $P_{k+1|k}$ can be obtained as follows

$$\begin{aligned} P_{k+1|k} &= \left(\overline{\gamma}_k - L_k \overline{\delta}_k\right) P_{k|k-1} \left(\overline{\gamma}_k - L_k \overline{\delta}_k\right)^T + E\left\{\left(\Delta\underline{\gamma}_k - L_k \Delta\underline{\delta}_k\right) q_k \left(\Delta\underline{\gamma}_k - L_k \Delta\underline{\delta}_k\right)^T\right\} \\ &+ E\left\{\Delta\underline{\eta}_{1,k} \underline{u}_k \underline{u}_k^T \Delta\underline{\eta}_{1,k}^T\right\} + E\left\{\underline{\eta}_{2,k} Q_{\underline{w}} \underline{\eta}_{2,k}^T\right\} + E\left\{\left(\Delta\underline{\gamma}_k - L_k \Delta\underline{\delta}_k\right) \underline{x}_k \underline{u}_k^T \Delta\underline{\eta}_{1,k}^T\right\} \\ &+ E\left\{\left(\Delta\underline{\gamma}_k - L_k \Delta\underline{\delta}_k\right) \underline{x}_k \underline{u}_k^T \Delta\underline{\eta}_{1,k}^T\right\}^T - E\left\{\underline{\eta}_{2,k} Q_s L_k^T\right\} - E\left\{\underline{\eta}_{2,k} Q_s L_k^T\right\}^T + L_k Q_{\underline{v}} L_k^T \end{aligned} \tag{37}$$

where

$$E\left\{\left(\Delta\underline{\gamma}_k - L_k\Delta\underline{\delta}_k\right)q_k\left(\Delta\underline{\gamma}_k - L_k\Delta\underline{\delta}_k\right)^T\right\}$$
$$= \left(\bar{b} - \bar{b}^2\right)(\Xi_1 - L_k\Xi_5)q_k(\Xi_1 - L_k\Xi_5)^T \tag{38}$$
$$+ \bar{b}\mathrm{Q}_\sigma(\Xi_2 - L_k\Xi_6)q_k(\Xi_2 - L_k\Xi_6)^T + \left(\bar{a} - \bar{a}^2\right)\Xi_3 q_k\Xi_3^T$$

$$E\left\{\Delta\underline{\eta}_{1,k}\underline{u}_k\underline{u}_k^T\Delta\underline{\eta}_{1,k}^T\right\} = \left(\bar{a} - \bar{a}^2 + \bar{a}Q_\omega\right)\Xi_4\underline{\bar{u}}_k\underline{\bar{u}}_k^T\Xi_4^T \tag{39}$$

$$E\left\{\underline{\eta}_{2,k}Q_{\underline{w}}\underline{\eta}_{2,k}^T\right\} = \underline{\bar{\eta}}_{2,k}Q_{\underline{w}}\underline{\bar{\eta}}_{2,k}^T \tag{40}$$

$$E\left\{\left(\Delta\underline{\gamma}_k - L_k\Delta\underline{\delta}_k\right)\underline{x}_k\underline{u}_k^T\Delta\underline{\eta}_{1,k}^T\right\} = \left(\bar{a} - \bar{a}^2\right)\Xi_3\underline{\bar{x}}_k\underline{\bar{u}}_k^T\Xi_4^T \tag{41}$$

$$E\left\{\underline{\eta}_{2,k}Q_sL_k^T\right\} = \underline{\bar{\eta}}_{2,k}Q_sL_k^T \tag{42}$$

Substituting Equations (38)–(42) into (37) results in prediction error covariance matrix.

According to Equation (18), the estimation error can be expressed as $\underline{\tilde{x}}_{k|k} = \underline{\tilde{x}}_{k|k-1} - K_k\Phi_k$, the filter error covariance matrix $P_{k|k}$ is derived as

$$P_{k|k} = P_{k|k-1} - K_k\theta_kK_k^T - K_kE\left\{\Phi_k\underline{\tilde{x}}_{k|k-1}^T\right\} - E\left\{\underline{\tilde{x}}_{k|k-1}\Phi_k^T\right\}K_k^T \tag{43}$$

where

$$E\left\{\underline{\tilde{x}}_{k|k-1}\Phi_k^T\right\} = E\left\{\underline{x}_{k|k}\Phi_k^T\right\} = K_k\theta_k \tag{44}$$

From Equations (43) and (44), it follows that

$$P_{k|k} = P_{k|k-1} - K_k\theta_kK_k^T \tag{45}$$

□

Remark 2. *The estimation-error covariance matrices $\{P_{k|k}\}$ and $\{P_{k+1|k}\}$ obey coupled iterative recursions. Drawing on the analysis framework in ref. [38], under suitable conditions: the iteration-domain dynamics satisfy detectability, packet-dropout probabilities $\bar{a}, \bar{b}$ are moderate, and the variances of multiplicative quantization noise and additive channel noise are bounded, the covariance sequences $\{P_{k|k}\}$ and $\{P_{k+1|k}\}$ are uniformly bounded and convergent with increasing iteration index k. Full detailed matrix-algebra derivation is omitted to keep manuscript concise. Note that an explicit bound relating plant tracking error to input estimation error is not derived here and will be studied in our future work.*

Note that the proposed approach does not adopt the conventional lifted representation which stacks all time-step samples of one trial. The filtering-state vector is formed by coupling ILC iteration evolution and signal transmission dynamics. Its dimension depends only on the plant's input-output channel number and does not increase with trial length. Fixed-dimension matrix recursions are performed at each instant, making the algorithm applicable for long-duration trials. Additionally, if we intend to extend the packet-dropout model from Bernoulli to Markov-type burst dropouts, several essential modifications are required. First, the channel stochastic model should be rebuilt with Markov state-transition rules to capture temporal correlation among packet dropouts. Second, the coupled iterative recursion for estimation-error covariance needs full reformulation to accommodate correlated channel noise. Third, the sufficient conditions for uniform boundedness and convergence of covariance sequences should be re-established accordingly. This valuable extension will be investigated in our future work.

4. Simulation Results

To verify the effectiveness of the proposed estimation method, a class of linear discrete-time plants are presented as follows:

$$\begin{cases} x_k(t+1) = Ax_k(t) + Bu_k^r(t) \\ y_k(t) = Cx_k(t) \end{cases}$$

where $x_k(t)$ and $y_k(t)$ represent the plant state and output sent to the controller, respectively; $u_k^r(t)$ is the received input; $t \in [0, 100]$ denotes the discrete time instant; and k is the iteration index. Matrices A, B, and C are given by

$$A = \begin{bmatrix} -0.5 & 0 & 0 \\ 1 & 1.24 & 0.87 \\ 0 & 0.87 & 0 \end{bmatrix}, B = \begin{bmatrix} 1 \\ 0 \\ 0 \end{bmatrix}, C = \begin{bmatrix} 2 \\ 2.6 \\ -2.8 \end{bmatrix}^T$$

The ILC controller given in (1) is adopted. The output tracking error is defined as $e_k(t+1) = y_d(t+1) - y_k(t+1)$. The desired trajectory is

$$y_d(t) = 10\left(1 + \sin\left(\frac{2\pi t}{100} - \frac{\pi}{2}\right)\right)$$

where the period is set as $T = 100$ in this simulation.

The learning gain is 0.12 that ensures the system convergence without communication constraints. The quantization density is chosen as $\rho = 0.8$. According to $\psi = (1-\rho)/(1+\rho)$, we obtain $\psi \approx 0.1111$. Consistent with the theoretical assumption, the multiplicative quantization noises $\omega_k(t)$ and $\sigma_k(t)$ are generated as zero-mean uniform random variables over $[-\psi, \psi]$ in simulation, which gives $Q_\omega = Q_\sigma = 0.004$. The means of data dropouts are set as $\bar{a} = \bar{b} = 0.96$, and the variances of zero-mean channel additive noises are given as $Q_m = Q_n = 0.06$. For the proposed estimator, the initial predicted state is $\hat{\underline{x}}_{0|-1} = \begin{bmatrix} 1 & 1 & 1 \end{bmatrix}^T$, and the initial prediction error covariance matrix is $P_{0|-1} = 0.1I_3$, where I_3 denotes the third-order identity matrix. This initialization will affect the transient estimation and tracking performance in the first few iterations. Additionally, the convergent input under the ideal communication environment is shown as the desired input for comparison, and the data compensation method and the standard Kalman filtering method are adopted as two benchmarks. For the data compensation method, if packet dropout occurs at time instant t in iteration k, the missing data is replaced by the received data at the same time instant t from iteration $k-1$. For the standard Kalman filter, it only considers additive Gaussian process noise and measurement noise and cannot jointly cope with logarithmic quantization and random packet dropouts. For fair comparison, the system matrices A, B, C and noise covariance matrices of both benchmark methods are set identical to those used in the proposed method. Convergence curves against iteration index are provided, where the Mean Absolute Error (MAE), i.e., the mean value of absolute tracking error within each trial, is taken as the evaluation index. Simulations under different packet-dropout probabilities are supplemented for robustness assessment.

Figure 2 shows the signal and error generated by the real logarithmic quantizer. It can be observed that practical quantization error is signal-dependent rather than ideal zero-mean noise. The tracking curves in Figures 3–10 are all plotted at the 25th iteration, where the proposed method has achieved stable convergence according to the convergence curves. Figures 3 and 4 display the raw input received by the plant and the output of this raw input. It can be seen that quantization errors, packet dropouts and channel noise lead to obvious fluctuations of the raw input. Correspondingly, the output of this raw input fails to track the desired output at the 25th iteration. Figures 5 and 6 show the input received with data compensation and the output of this input. It can be seen that the data

compensation has suppressed the fluctuations of the received input to a certain extent, but it cannot fully guarantee the convergence of the received input. The reason is that this method cannot simultaneously deal with the impact of quantization error and channel noise. Figures 7 and 8 illustrate the input estimated by the standard Kalman filter. Similar to the results shown in Figure 5, the standard Kalman filtering method only suppresses the fluctuations of input waveform to a certain extent, and accordingly, the output of this input cannot achieve accurate tracking of the desired trajectory. The reason is that the standard Kalman filtering method can only deal with the impact of channel noise, but cannot deal with the impact of quantization error and packet dropouts. Figures 9 and 10 display the input obtained by the proposed estimation method and the output of the input, respectively. It can be seen from the figures that thanks to the proposed estimation method, the input curve can track the desired input at the 25th iteration, and naturally, the output of the input also converges to the desired output. The reason is that the proposed estimation method considers the effects of quantization errors, packet dropouts and channel noise at the same time when establishing the estimation model.

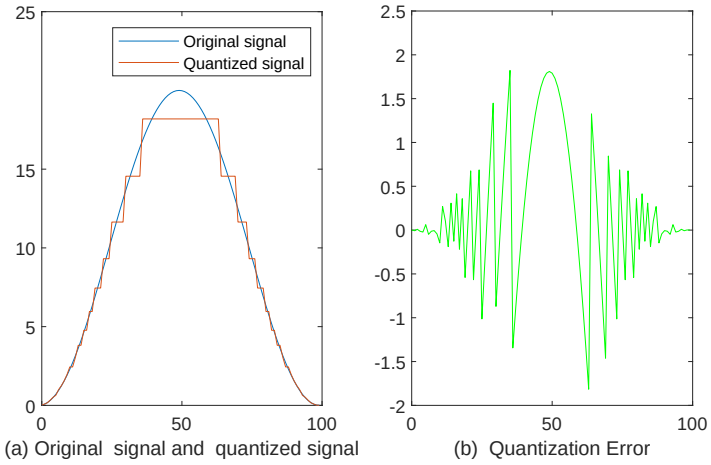


Figure 2. Illustration of logarithmic quantization.

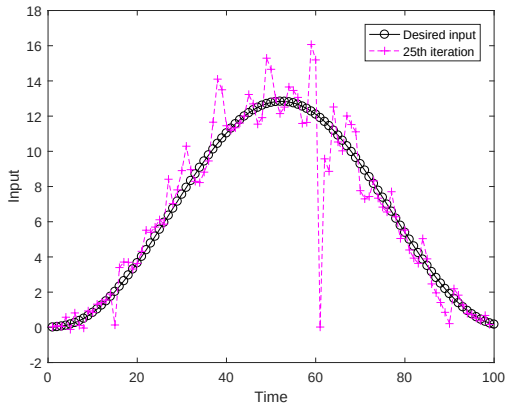


Figure 3. The raw input.

In order to further verify the effectiveness of the proposed method, the convergence of input and output is investigated by taking the MAE within each iteration as the evaluation index. The curves in Figures 11 and 12 are from a single realization. For each iteration k, the MAE over all discrete time instants within this iteration is calculated, and random disturbances are generated at each time step. It can be seen from Figures 11 and 12 that the MAE of raw input error and the corresponding output error exhibit the poorest conver-

gence. The packet-dropout compensation method and the conventional Kalman filter can achieve approximate convergence. Compared with the raw case, both methods improve the convergence performance to a certain degree, yet they cannot guarantee full convergence. In contrast, only the proposed method achieves fully convergent MAEs of input and output errors, which further demonstrates the effectiveness of our method.

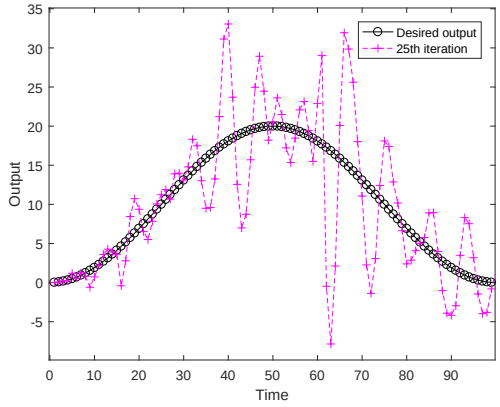


Figure 4. The output of raw input.

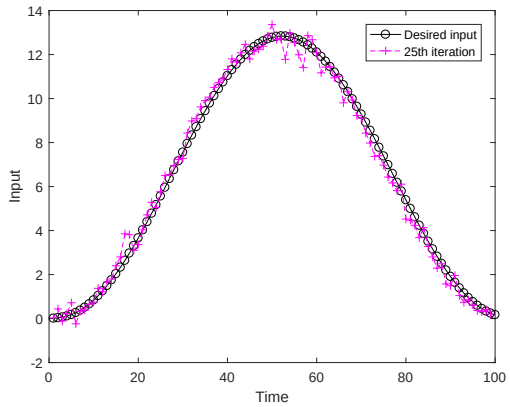


Figure 5. The input with data compensation.

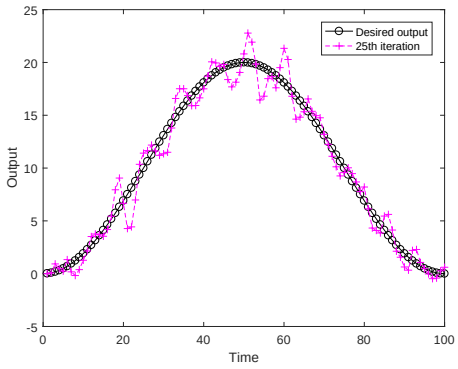


Figure 6. The output of input with data compensation.

To test the robustness against channel-parameter variations, simulations under different packet-dropout rates (corresponding to transmission success probabilities of 0.99, 0.96 and 0.93) are carried out to evaluate estimation and tracking performance. Figures 13 and 14 show the evolution of input and output MAEs versus iteration index under transmission success

probabilities of 0.99, 0.96 and 0.93. The convergence speed is the highest at 0.99 and lowest at 0.93. Since the control input converges in the iteration domain and the packet-dropout compensation scheme utilizes the correctly received data at the same instant from the prior iteration, larger packet dropout rates result in slower convergence.

Additional statistical Monte Carlo results, ablation tests and quantization sensitivity analysis are provided in the Supplementary Materials for further validation.

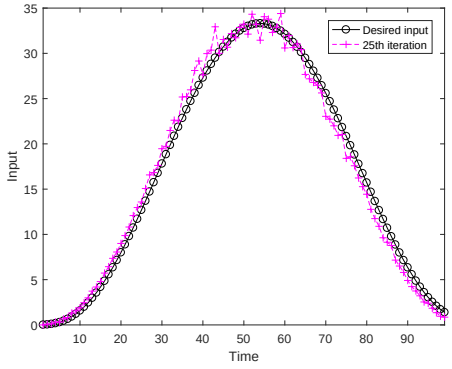


Figure 7. The input estimated by the standard Kalman filter.

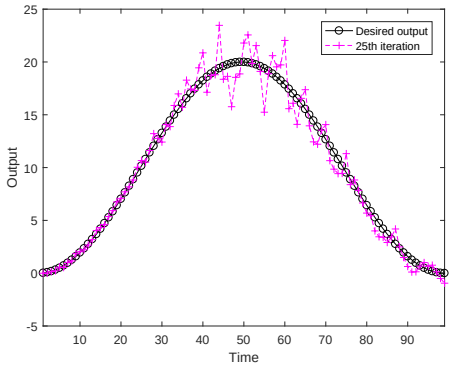


Figure 8. The output of input estimated by the standard Kalman filter.

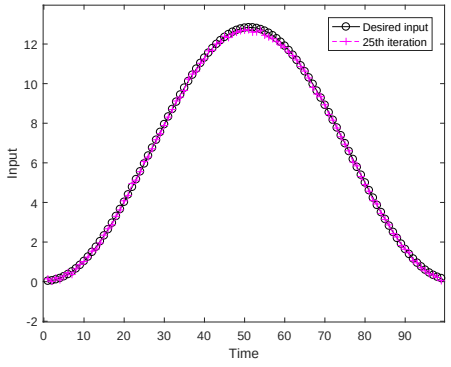


Figure 9. The input estimated by the proposed estimator.

https://doi.org/10.3390/math14213981

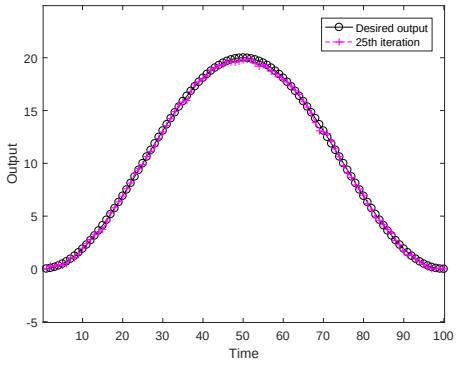


Figure 10. The output of input estimated by the proposed estimator.

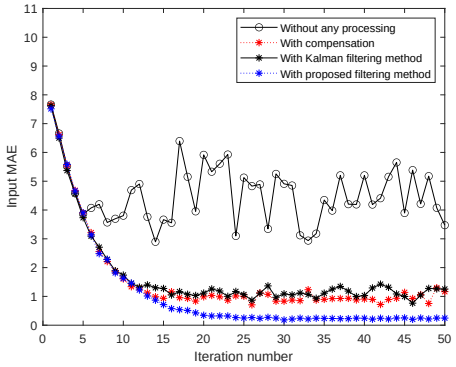


Figure 11. Comparison of input MAE under different methods.

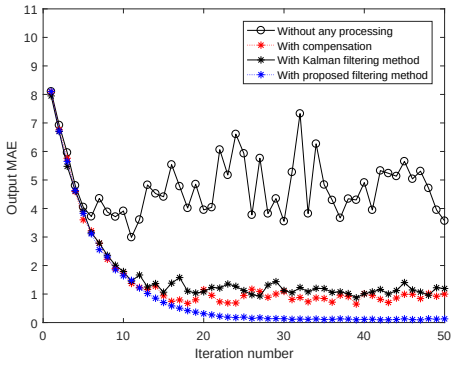


Figure 12. Comparison of output MAE under different methods.

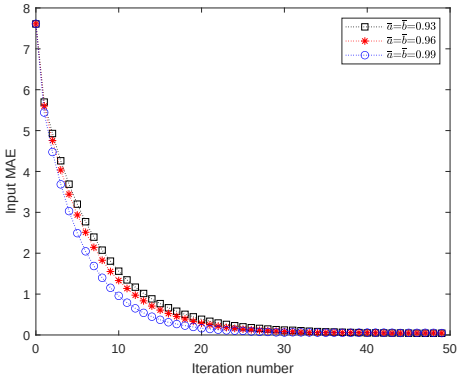


Figure 13. Comparison of input MAE under different dropout probabilities.

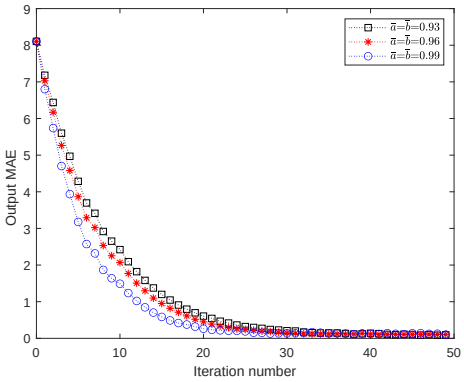


Figure 14. Comparison of output MAE under different dropout probabilities.

5. Conclusions

This paper investigates the input estimation problem for networked ILC systems suffering from logarithmic quantization and random packet dropouts. Different from existing methods that redesign ILC update laws, this work develops a plant-side estimation framework to reconstruct the actual control input without modifying the original learning strategy. Within the tested scenarios, the proposed framework can suppress quantization-induced multiplicative noise and packet-dropout data distortion. Numerical simulations illustrate the uniform boundedness and convergence of estimation error covariance observed in these tests, and demonstrate improved tracking performance compared with the iteration-domain data compensation method and the conventional Kalman filtering method.

Nevertheless, this work still has several limitations. First, packet dropouts are modeled as Bernoulli independent events, which ignores temporal channel correlation and burst dropout characteristics in practical wireless links. Second, the channel noise and quantization statistics are assumed known and iteration-independent, while practical repetitive systems may contain iteration-varying or iteration-correlated disturbances. Third, the stochastic equivalent multiplicative quantization model may introduce conservativeness when the control signal approaches the quantizer dead zone.

Future work will focus on the following concrete extensions. First, the packet-dropout model will be generalized to Markov burst dropout processes to accommodate correlated wireless channel fading. Second, parameter mismatch and iteration-correlated disturbances will be considered to improve the algorithm robustness. Third, joint design of learning law and state estimation will be further explored to achieve higher tracking accuracy under complex network environments.

Supplementary Materials: The following supporting information can be downloaded at: https://www.mdpi.com/article/10.3390/math14213981/s1, Figure S1: Without-processing scheme: Input MAE and Output MAE; Figure S2: Iteration-domain compensation: Input MAE and Output MAE; Figure S3: Standard Kalman filter: Input MAE and Output MAE; Figure S4: Proposed estimator: Input MAE and Output MAE; Figure S5: Only packet dropouts: Input MAE and Output MAE; Figure S6: Only quantization errors: Input MAE and Output MAE; Figure S7: Varying quantization steps: Input MAE and Output MAE.

Author Contributions: Conceptualization, H.N. and Z.D.; methodology, H.N. and Z.D.; writing—original draft, H.N., Z.D. and L.H.; writing—review & editing, H.N., Z.D. and L.H. All authors have read and agreed to the published version of the manuscript.

Funding: This work was supported by the Natural Science Foundation of Henan Province [Grant No. 252300421517].

Data Availability Statement: The original contributions presented in the study are included in the article and Supplementary Materials, further inquiries can be directed to the corresponding author.

Conflicts of Interest: The authors declare no conflict of interest.

References

1. Cai, G.; Yin, G.; Liu, Y.; Feng, J.; Liang, J.; Wang, F.; Liu, H. Stochastic cooperative adaptive cruise control with sensor data distortion and communication delay. *IEEE Trans. Intell. Transp. Syst.* **2025**, *26*, 9500–9515. [CrossRef]
2. Ngo, V.T.; Liu, Y.C. Control strategies for robot-assisted telerehabilitation under communication delay: A survey. *Asian J. Control* **2026**, 639–646. [CrossRef]
3. Ding, L.; Han, Q.; Sindi, E.; Wang, L.Y. Distributed cooperative optimal control of DC microgrids with communication delays. *IEEE Trans. Ind. Inform.* **2018**, *14*, 3924–3935. [CrossRef]
4. Dai, D.; Li, J.; Li, H.; Dong, H.; Li, H.; Xu, G. Recursive filtering for an uncertain system with wireless switching channels and fading measurements: A microseismic event detection method. *Syst. Control Lett.* **2024**, *183*, 105692. [CrossRef]
5. Chen, K.; Yuan, X.; Wang, J. Adaptive iterative learning control for upper limb rehabilitation robots considering unknown disturbance. *Eur. J. Control* **2026**, *89*, 101507. [CrossRef]
6. Tian, T.; Sun, S. Fusion estimation against mixed network attacks for systems with random parameter matrices, correlated noises, and quantized measurements. *Digit. Signal Process.* **2024**, *150*, 104523. [CrossRef]
7. Liu, S.; Wang, Z.; Hu, J.; Wei, G. Protocol-based extended Kalman filtering with quantization effects: The Round-Robin case. *Int. J. Robust Nonlinear Control* **2020**, *30*, 7927–7946. [CrossRef]
8. Liu, Q.; Wang, Z.; Han, Q.; Jiang, C. Quadratic estimation for discrete time-varying non-Gaussian systems with multiplicative noises and quantization effects. *Automatica* **2020**, *113*, 108714. [CrossRef]
9. Wang, L.; Wang, Z.; Wei, G.; Alsaadi, F.E. Observer-based consensus control for discrete-time multiagent systems with coding–decoding communication protocol. *IEEE Trans. Cybern.* **2018**, *49*, 4335–4345. [CrossRef] [PubMed]
10. Lu, R.; Tao, J.; Shi, P.; Su, H.; Wu, Z.G.; Xu, Y. Dissipativity-based resilient filtering of periodic Markovian jump neural networks with quantized measurements. *IEEE Trans. Neural Netw. Learn. Syst.* **2017**, *29*, 1888–1899. [CrossRef] [PubMed]
11. Chen, J.; Hua, C.; Guan, X. Iterative learning model-free control for networked systems with dual-direction data dropouts and actuator faults. *IEEE Trans. Neural Netw. Learn. Syst.* **2020**, *32*, 5232–5240. [CrossRef] [PubMed]
12. Bu, X.; Hou, Z.; Jin, S.; Chi, R. An iterative learning control design approach for networked control systems with data dropouts. *Int. J. Robust Nonlinear Control* **2016**, *26*, 91–109. [CrossRef]
13. Chi, R.; Lv, Y.; Hou, Z. Compensation-based data-driven ILC with input and output package dropouts. *Int. J. Robust Nonlinear Control* **2020**, *30*, 950–965. [CrossRef]
14. Liu, J.; Ruan, X. Networked iterative learning control design for nonlinear systems with stochastic output packet dropouts. *Asian J. Control* **2018**, *20*, 1077–1087. [CrossRef]
15. Tao, Y.; Tao, H.; Zhuang, Z.; Stojanovic, V.; Paszke, W. Quantized iterative learning control of communication-constrained systems with encoding and decoding mechanism. *Trans. Inst. Meas. Control* **2024**, *46*, 1943–1954. [CrossRef]
16. Huang, L.; Sun, L.; Wang, T.; Liu, W.; Zhang, Z.; Zhang, Q. Optimal input filters for iterative learning control systems with additive noises, random delays, and data dropouts in both channels. *Math. Methods Appl. Sci.* **2022**, *45*, 4295–4311. [CrossRef]
17. Huang, L.; Chen, H.; Sun, L.; Jiang, B.; Zhang, Y.; Zhang, Q. An estimator for input sent by ILC controllers through multi-path fading channels. *Int. J. Control Autom. Syst.* **2024**, *22*, 3459–3471. [CrossRef]
18. Wang, F.; Wang, Z.; Liang, J.; Liu, X. Resilient filtering for linear time-varying repetitive processes under uniform quantizations and Round-Robin protocols. *IEEE Trans. Circuits Syst. I* **2018**, *65*, 2992–3004. [CrossRef]
19. Liu, S.; Wei, G.; Song, Y.; Ding, D. Set-membership state estimation subject to uniform quantization effects and communication constraints. *J. Frankl. Inst.* **2017**, *354*, 7012–7027. [CrossRef]
20. Niu, Y.; Sheng, L. Uniform quantized synchronization for chaotic neural networks with successive packet dropouts. *Asian J. Control* **2019**, *21*, 639–646. [CrossRef]
21. Gong, C.; Zhu, G.; Shi, P. Secure and asynchronous filtering for piecewise homogeneous Markov jump systems with quantization and Round-Robin communication. *Inf. Sci.* **2023**, *640*, 119032. [CrossRef]
22. Wang, S.; Tian, X.; Fang, H. Event-based state and fault estimation for nonlinear systems with logarithmic quantization and missing measurements. *J. Frankl. Inst.* **2019**, *356*, 4076–4096. [CrossRef]
23. Hua, M.; Zhang, F.; Deng, F.; Fei, J.; Chen, H. H_∞ filtering for discrete-time periodic Markov jump systems with quantized measurements: A new packet loss compensation strategy. *IEEE Trans. Syst. Man Cybern. Syst.* **2023**, *53*, 6766–6777. [CrossRef]
24. Dong, S.; Su, H.; Shi, P.; Lu, R.; Wu, Z.G. Filtering for discrete-time switched fuzzy systems with quantization. *IEEE Trans. Fuzzy Syst.* **2016**, *25*, 1616–1628. [CrossRef]

25. Mao, J.; Ding, D.; Wei, G.; Liu, H. Networked recursive filtering for time-delayed nonlinear stochastic systems with uniform quantisation under Round-Robin protocol. *Int. J. Syst. Sci.* **2019**, *50*, 871–884. [CrossRef]
26. Fu, M.; Xie, L. The sector bound approach to quantized feedback control. *IEEE Trans. Autom. Control* **2005**, *50*, 1698–1711. [CrossRef]
27. Huang, L.; Wang, H.; Sun, L.; Chen, T.; Zhang, Q.; Liu, W.; Zhang, Y. Method for predicting the lost input of iterative learning control systems over AWGN channels. *J. Differ. Equ. Appl.* **2024**, *30*, 1885–1899. [CrossRef]
28. Baigzadehnoe, B.; Rezaie, B.; Rahmani, Z. Fuzzy-model-based fault detection for nonlinear networked control systems with periodic access constraints and Bernoulli packet dropouts. *Appl. Soft Comput.* **2019**, *80*, 465–474. [CrossRef]
29. Li, J.; Lu, R.; Xu, Y.; Peng, H.; Rao, H.X. Distributed state estimation for periodic systems with sensor nonlinearities and successive packet dropouts. *Neurocomputing* **2017**, *237*, 50–58. [CrossRef]
30. Liu, Y.; Yang, W.; Zhou, J.; Luo, Y. H_∞ filter for discrete-time periodic piecewise systems with missing measurements. *IEEE Trans. Syst. Man Cybern. Syst.* **2023**, *53*, 5648–5657. [CrossRef]
31. Cetinkaya, A.; Ishii, H.; Hayakawa, T. Networked control under random and malicious packet losses. *IEEE Trans. Autom. Control* **2016**, *62*, 2434–2449. [CrossRef]
32. Hervé, S.A.; Aurelien, Y.T.; Leandre, N.N. Optimal PD-type networked iterative learning algorithm based fault estimation for repetitive systems with delays, packet losses, sensor saturation and sensor failure. *Int. J. Dyn. Control* **2022**, *10*, 1062–1074. [CrossRef]
33. Hu, J.; Zhang, P.; Kao, Y.; Liu, H.; Chen, D. Sliding mode control for Markovian jump repeated scalar nonlinear systems with packet dropouts: The uncertain occurrence probabilities case. *Appl. Math. Comput.* **2019**, *362*, 124574. [CrossRef]
34. Sun, S.; Li, X. Robust networked ILC for switched nonlinear discrete systems with non-repetitive uncertainties and random data dropouts. *Int. J. Syst. Sci.* **2021**, *52*, 1746–1760. [CrossRef]
35. Guo, X.; Huang, L.; Sun, L.; Liu, W.; Zhang, Z.; Zhang, Q. Optimal state filters for networked iterative learning control systems with data losses and noises. *Int. J. Adapt. Control Signal Process.* **2024**, *38*, 1528–1542. [CrossRef]
36. Wang, W.; Cao, L.; Pan, Y.; Ren, H.; Xue, H. Self-triggered adjustable prescribed performance control for stochastic multiagent systems with communication faults. *Appl. Intell.* **2024**, *54*, 3058–3076. [CrossRef]
37. Huang, L.; Fang, Y.; Wang, T. Convergence analysis of wireless remote iterative learning control systems with channel noise. *Asian J. Control* **2015**, *17*, 2374–2381. [CrossRef]
38. Huang, L.; Sun, L.; Wang, T.; Zhang, Q.; Li, J.; Zhang, Z.; Liu, W. Optimal input filtering for networked iterative learning control systems with packet dropouts and channel noises in both sides. *Int. J. Robust Nonlinear Control* **2022**, *32*, 5086–5104. [CrossRef]
39. Muramatsu, H.; Katsura, S. An adaptive periodic-disturbance observer for periodic-disturbance suppression. *IEEE Trans. Ind. Inform.* **2018**, *14*, 4446–4456. [CrossRef]
40. Zhang, Z.; Lin, D.; Wang, X.; Shao, Z.; Lin, W. A periodic event-triggered design of robust filtering for T-S fuzzy discrete-time systems. *Front. Neurosci.* **2019**, *13*, 318. [CrossRef] [PubMed]

Disclaimer/Publisher's Note: The statements, opinions and data contained in all publications are solely those of the individual author(s) and contributor(s) and not of MDPI and/or the editor(s). MDPI and/or the editor(s) disclaim responsibility for any injury to people or property resulting from any ideas, methods, instructions or products referred to in the content.